

POLITECNICO DI TORINO
Repository ISTITUZIONALE

Transmission of 61 C-band Channels with L-band Interferers over Record 618km of Hollow-Core-Fiber

Original

Transmission of 61 C-band Channels with L-band Interferers over Record 618km of Hollow-Core-Fiber / Nespolo, A; Straullu, S; Bradley, Td; Harrington, K; Sakr, H; Jasion, Gt; Fokoua, En; Jung, Ym; Chen, Y; Hayes, Jr; Forghieri, F; Richardson, Dj; Poletti, F; Bosco, G; Poggolini, P. - ELETTRONICO. - (2020). (Intervento presentato al convegno Optical Fiber Communications Conference and Exhibition (OFC) tenutosi a San Diego (CA), USA nel 8-12 March 2020).

Availability:

This version is available at: 11583/2948082 since: 2022-02-27T19:45:02Z

Publisher:

IEEE

Published

DOI:

Terms of use:

This article is made available under terms and conditions as specified in the corresponding bibliographic description in the repository

Publisher copyright

IEEE postprint/Author's Accepted Manuscript

©2020 IEEE. Personal use of this material is permitted. Permission from IEEE must be obtained for all other uses, in any current or future media, including reprinting/republishing this material for advertising or promotional purposes, creating new collecting works, for resale or lists, or reuse of any copyrighted component of this work in other works.

(Article begins on next page)

Transmission of 61 C-band Channels with L-band Interferers over Record 618km of Hollow-Core-Fiber

Antonino Nespoli¹, Stefano Straullu¹, Thomas D Bradley², Kerrianne Harrington², Hesham Sakr², Gregory T Jasion², Eric Numkam Fokoua², Yongmin Jung², Yong Chen², John R Hayes², Fabrizio Forghieri⁴, David J Richardson², Francesco Poletti², Gabriella Bosco³, Pierluigi Poggolini³

¹LINKS Foundation, 10129, Torino, Italy; ²Optoelectronics Research Centre, University of Southampton, SO17 1BJ, UK

³OptCom, DET, Politecnico di Torino, 10129, Torino, Italy; pierluigi.poggolini@polito.it

⁴CISCO Photonics, Vimercate (MB), Italy

Abstract: We recirculated 61 PM-QPSK C-band channels @32GBaud, with simultaneous L-band loading, through 7.72km of hollow-core NANF with <1dB/km loss. We reached 772km for the mid-channel, and 618km for all channels at average GMI 3.44 bits/symbol.

1. Introduction

Light transmission in a hollow-core fiber (HCF) promises many advantages over transmission through conventional glass-core fiber: lower nonlinearity, latency and backscattering and less sensitivity to perturbations [1]. Amongst numerous potential applications, data transmission is arguably the most impactful goal for the technology. Early data transmission experiments performed on 100-300 meters of photonic band-gap HCFs (PBGFs), progressed from single channel 10Gbit/s OOK [2] to 40Gbit/s DWDM [3], up to high data throughput (76Tbit/s) exploiting 256QAM with polarization and mode multiplexing [4]. Meanwhile, other studies assessed the transmission potential of PBGFs through longer-distances: 2.75km using a commercial 100G interface [5] and a single channel 20Gbit/s QPSK over an 11km span with 66dB loss [6]. When PBGFs were first inserted in a recirculating loop to test their performance over even longer distances however, the fairly large intermodal cross-talk in these fibers appeared as rather limiting. 74.8km transmission was achieved by recirculating a single 28GBaud QPSK channel (with two untested side channels added for spectral equalization) 12 times through a span comprising 6.2km (48.1dB loss) of PBGF [7].

A considerable improvement in performance was obtained by switching to a different type of HCF, the Nested Antiresonant Nodeless Fiber (NANF) [8]. The NANF not only produces considerably lower losses (current record: 0.65dB/km [9]), and broader 3dB bandwidths (700nm in [10]) than data-transmitting PBGFs, but thanks to an inherent and distributed high-order mode stripping mechanism, NANFs can also considerably reduce the intermodal interference (IM-I) that impairs long distance data transmission. In the current transmission distance record (341km), 71 re-circulations through a 4.8km assembled span of NANF were achieved by a PM-QPSK 32GBaud channel, propagating at the center of a 61-channel WDM comb, at a pre-FEC BER of less than 3e-2 [11]. However, only the center channel was measured, and the full WDM transmission was not tested.

In this work, we managed to produce and assemble the longest NANF transmission line yet constructed (7.72km), obtained by splicing the longest continuous length of NANF so far reported, 4.34km, to another 3.38km long band. The average estimated NANF loss at 1550nm through the whole span was as low as 0.84dB/km. The total insertion loss of the assembled NANF line, including NANF/NANF and NANF/SMF splices, was 9.1dB. The NANF transmission line was placed into a recirculating loop that carried 61 PM-QPSK 32GBaud C-band DWDM channels. The NANF was also loaded with 61x32GBaud non-recirculating interferers in the L-band, to check for possible cross-band effects. Setting a threshold GMI of 3.55 bits/symbol, the center channel reached 772km (100 recirculations), more than twice the previous directly comparable record [11]. We also achieved 80 recirculations (618km) at a GMI average across all DWDM channels of 3.44 bits/symb. These results represent the longest transmission distances ever reported over *any* HCF (Fig.1(a)) and show that very significant progress has been made towards potential future HCF use in long-haul high-capacity terrestrial systems.

2. Assembly of a 7.72km NANF span

NANFs from two separate draws and different preforms, both designed to operate in the 1st antiresonant window, were spliced together to form a 7.72km assembled line. Their scanning electron micrographs (SEMs) are shown in Fig.1(b). The two fibers are geometrically similar, with a difference in the size of their inner tubes. NANF1 (3.38km), also employed in the previous experiment [11], has an average core diameter, membrane thickness and length of 35.6µm, 0.55µm and 3.38km, respectively. Its loss (Fig.1(c)) decreases from 1.37dB/km at 1530nm to 1.15dB/km at 1625nm (1.30dB/km at 1550nm). NANF2 was fabricated with similar core diameter and membrane thickness (35.9µm, 0.48 µm). However, by finessing the fabrication recipes we produced the longest NANF span from a single draw to date (4.34 km). In addition, NANF2 has a considerably lower loss (0.82 dB/km, Fig.1(c)) than NANF1, spectrally flat from

1530 to 1625nm and not far from the record 0.65dB/km reported in [9]. The loss curves of both NANFs shown in Fig.1(c) were measured by cutting back the fibers to 10m. The measured loss of the assembled NANF line was 8.7dB. Besides the NANFs, loss was due to splicing to SMF patchcords using mode field adapters (~1dB loss per end) and to the mid-span NANF-NANF splice (~0.2dB). Interestingly, taking out splice loss, the spooled NANF estimated pure propagation loss was lower than suggested by the cutback measurements, ~6.50dB total or ~0.84dB/km average.

Preliminary experiments indicated that the smaller tubes in NANF 1 (9.88 μ m) produced noticeably less IM-I than NANF2 (13.27 μ m). To mitigate the in-band IM-I, mostly caused by NANF2, we introduced high-order mode stripping loops. Loops with 5 turns of 4.8cm bend diameter were added to NANF1 at the launch and before the splice joining NANF1 to NANF2, and 5 loops of 7.3cm bend diameter were added in NANF2 after this splice, adding ~0.4dB loss and raising the total insertion loss to 9.1dB, but considerably reducing cross-talk and improving the loop performance.

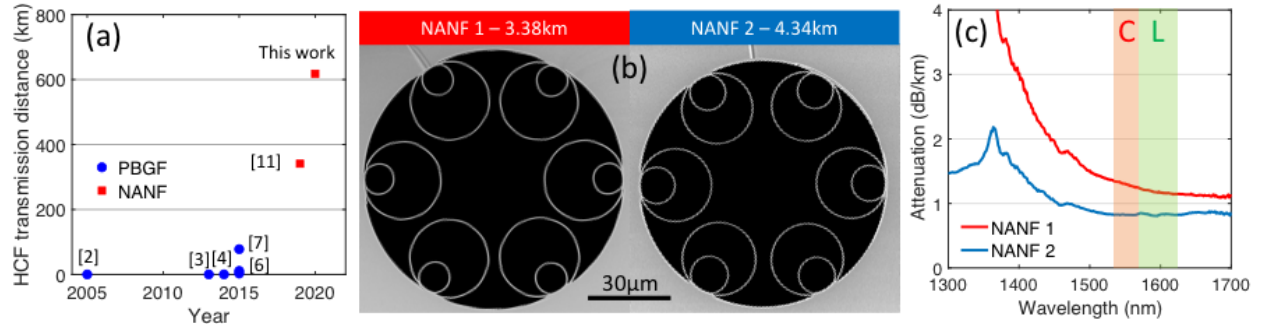


Fig.1: (a) Evolution of data transmission distance through HCFs; (b) cross sectional SEMs of the two fibers; (c) Cutback loss.

3. Recirculating loop experiment

A total of 122 DWDM channels (61 C-band and 61 L-band) were emulated by shaping ASE noise as raised-cosine spectra with 32 GHz bandwidth, 0.2 roll-off and 50 GHz spacing (Fig.2(a)). This was done by means of high-resolution programmable filters (Finisar Waveshapers). For transmission performance measurements, in turn each one of the 61 ASE-emulated C-band channels was turned off and replaced by an actual modulated Channel Under Test (CUT). The C-band transmitter schematic is shown in Fig.2(b). The CUT used a <100kHz External Cavity Laser (ECL) and was PM-QPSK modulated at 32GBaud by means of a dual-polarization Mach-Zehnder Modulator (MZM) driven by four 64GS/s DACs. The CUT spectrum was raised-cosine with 20%-roll-off. The back-to-back performance of the CUT is shown in Fig.2(c). At a pre-FEC BER of 3e-2 (or GMI 3.55 bits/symb), the back-to-back penalty was 0.65dB.

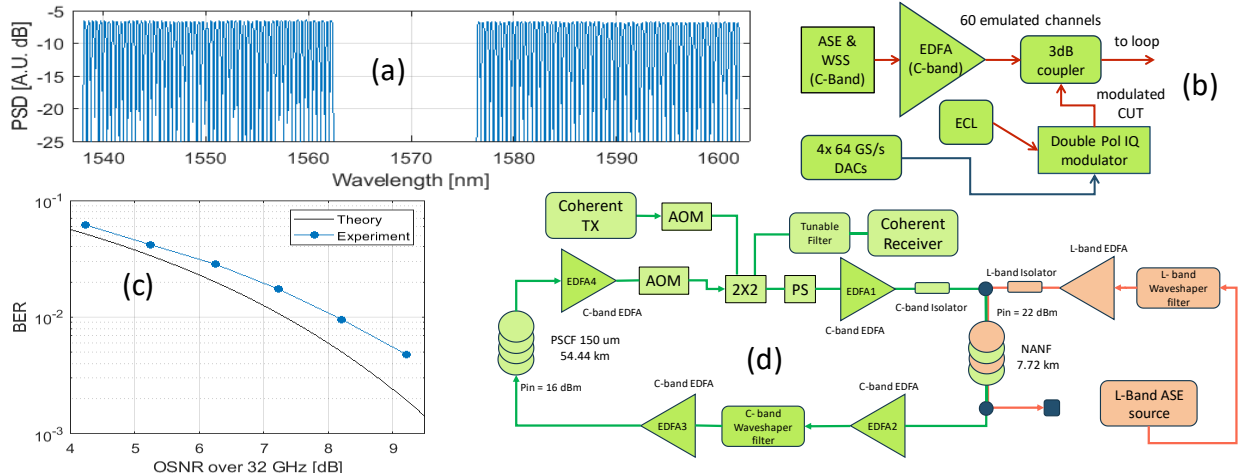


Fig. 2: (a) power spectral density (PSD) of the C+L 122-channel WDM spectrum (b) C-band transmitter schematic; (c) back-to-back BER vs. OSNR of the PM-QPSK Tx/Rx pair; (d) loop schematic (green C-band signal, pink L-band signal).

The loop schematic is shown in Fig.2(d). The loop re-circulated the C-band WDM comb, while the L-band comb went through the NANF without recirculating, as explained below. The loop consisted of four sections, each starting with an EDFA. EDFA1 launched the C-band WDM comb at 19dBm into the 7.72km NANF. It was followed by EDFA2 feeding a programmable filter tasked with flattening the overall loop transfer function, followed by EDFA3 and a spool of 55km of PSCF, followed by EDFA4 feeding an acousto-optic modulator, a 2x2 splitter/combiner and

a synchronous polarization scrambler (PS), the latter used to randomize the state of polarization at each re-circulation. The PSCF was necessary to provide sufficient signal loading capability and long-enough round-trip delay for loop management and stability. The EDFA3 launch power into the PSCF was set to 16 dBm, a value which kept the PSCF in linearity. Right before the NANF, a WDM combiner added the L-band WDM comb into the NANF. Immediately after the NANF a WDM splitter stripped out the L-band WDM comb from the loop. The L-band comb was launched into the NANF at the same power level as the C-band comb (see Fig. 2(a)), to test for possible cross-band interactions.

At the receiver, a tuneable optical filter selected the CUT, which was combined with a <100kHz ECL local-oscillator in an integrated coherent receiver. The four electrical outputs were sampled at 50 GS/s and offline processed. The DSP performed upsampling to 2 samp/symb, chromatic dispersion compensation and frequency offset removal. Next, the signal went through a complex 2×2 LMS adaptive equalizer, followed by a V&V CPE which used 5% pilot symbols to perform phase unwrapping and improve phase-recovery. Fig.3(a) shows the GMI-vs.-recirculations for the C-band center channel (#31). Assuming a threshold of 3.55 bits/symb (corresponding to a pre-FEC BER in AWGN of $3e-2$) the max-reach was 100 recirculations, corresponding to about 772km in NANF. The loop was then set to 80 recirculations, or 618km in NANF. Dots in Fig.3(b) show the GMI for each C-band channel, averaged over 6 measurements, taken on different days. Vertical bars range between min and max measured values. The mean GMI across all channels was 3.44 bits/symb. The results did not change when turning on or off the injection of the L-band comb, proving that the NANF does not cause any cross-band effect (such as ISRS), at least at these launch powers.

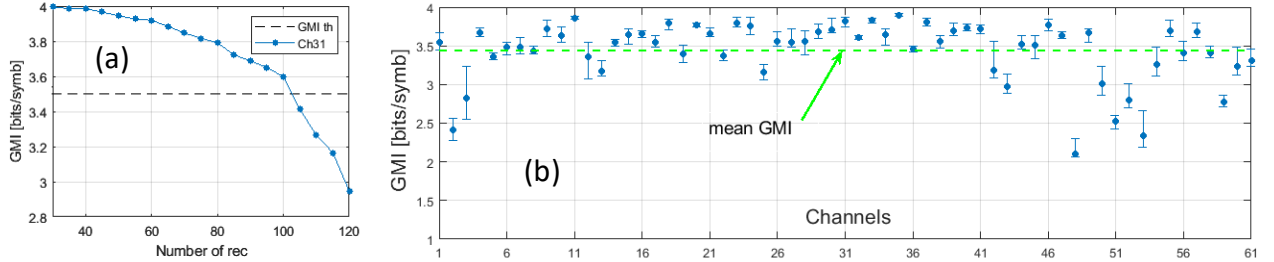


Fig. 3: (a) GMI-vs.-recirculations for the C-band center channel; (b) GMI for all C-band channels at 80 recirculations (618km).

As a control experiment, we replaced the NANF with an attenuator set to exactly match the NANF line attenuation (9.1dB). The center channel reached 215 recirculations at a GMI of 3.55 bits/symb. Channel uniformity was much better than with NANF, with all 61 channels above 3.55 bits/symb at 200 recirculations. We deem the main reason for the performance gap and channel non-uniformity of the NANF experiment vs. the VOA experiment to likely be IM-I. A strong indication in this respect was that we had to stretch the LMS equalizer filters impulse response length to 400 taps to maximize transmission performance when the NANF was in the loop. 60 taps were enough with the VOA.

4. Conclusion

Nested Antiresonant Nodeless Fibers (NANFs) have been making steady progress over the last few years, to the point that state-of-the-art NANFs can now be used in long-haul DWDM transmission experiments, a first for HCFs. In this paper we report on one such experiment, using 61 C-band transmission channels with 32GBaud PM-QPSK modulation and 61 L-band interferers. We achieved a record 618km transmission in NANF, at an overall average GMI of 3.44 bits/symb. This is 80% longer than the previous record (341km) [11], where however only the center channel had been measured (in this experiment the center channel actually reached 772km).

Our results also show that, besides loss, improvements are needed on the suppression of inter-modal interference, which seems possible with suitable design optimization (e.g. NANF1 performed much better than NANF2). If progress in NANF performance continues at the present rate, it might become a promising alternative in the quest for next-generation higher-throughput fibers, given its theoretical potential of achieving low loss and ultra-low non-linearity over ultra-wide bandwidths, ideally bringing about a many-fold increase in throughput per fiber [12].

This research was supported by the PhotoNext initiative of Politecnico di Torino, by the CISCO SRA OPTSYS-2020, by the European Research Council (ERC) (grant agreement n° 682724), by the EPSRC Airguide Photonics (EP/P030181/1), by Lumenisity and by the UK Royal Academy of Engineering. We also thank Lumentum Italy for supplying the dual-polarization MZ modulator.

- [1] R. F. Cregan et al., Science 285, 1537-1539, 1999.
- [2] C. Peucheret et al., Electron. Lett., Vol. 41, No. 1, p. 27, 2005.
- [3] F. Poletti et al., Nature Photon., vol. 7, pp. 279–284, 2013.
- [4] V. A. J. M. Sleijfer et al., J. Lightwave. Technol., vol. 32, no. 4, pp. 854–863, Feb. 2014.
- [5] M. Kuschnerov et al., J. Lightwave Technol., vol. 34, no. 2, pp. 314–320, Jan. 15, 2016.
- [6] Y. Chen et al., JLT., vol. 34, no. 1, pp. 104-113, Jan.1, 2016.
- [7] M.Kuschnerov et al., Proc ECOC 2015, paper Th1.2.4.
- [8] F. Poletti, Opt. Exp., vol. 22, pp. 23807–23828, 2014.
- [9] T.D. Bradley, et al., Proc. ECOC 2019, paper PD1.7.
- [10] H. Sakr, et al., Proc. OFC 2019, paper PDP Th4A.1.
- [11] A. Nespolà et al, Proc. ECOC 2019, paper PD.1.5.
- [12] F. Poletti, P. Poggolini, Proc. ECOC 2019, paper P51